Infrared Excitation Processes for the Visible Luminescence of Er^{3+}, Ho^{3+}, and Tm^{3+} in Yb^{3+}-Sensitized Rare-Earth Trifluorides

RALPH A. HEWES AND JAMES F. SARVER
Lighting Research Laboratory, Lamp Division, General Electric Company, Cleveland, Ohio 44112
(Received 5 December 1968)

Infrared reflectance and excitation measurements, together with studies of the dependence of the luminescence on excitation intensity and sensitizer concentration, in the fluorides of La, Gd, and Y doped with Yb^{3+} and Er^{3+}, Ho^{3+}, or Tm^{3+} indicate that infrared quantum counteraction is accomplished by absorption of energy in the Yb^{3+} ions followed by two (for Ho^{3+} or Er^{3+}) or three (for Tm^{3+}) transfers to the activator, resulting in production of strong visible luminescence from absorption in the Yb^{3+}($^2F_{7/2}$-$^2F_{5/2}$) band. Saturation of the population of intermediate levels, in the case of Tm^{3+}-activated materials, was observed and is believed to account for previous results which were interpreted as evidence of a so-called "cooperative sensitization," in which only two (simultaneous) transfers were required.

INTRODUCTION

THE concept of the infrared quantum counter (IRQC), originally due to Bloembergen,[1] in which a rare-earth ion is excited to a state giving rise to visible luminescence by the absorption of an infrared photon and another pump photon (necessarily distinguishable from the luminescence) has been broadened by the consideration of other rare-earth ions as sensitizers. In such a generalized system, part of the required absorption is accomplished by these other ions, which may or may not be identical to the luminescing or activator ions, and a portion of that energy is transferred by a resonance process to the activator. Self-sensitized systems involving only activator-activator transfer have been known for some time,[2–4] but systems in which the sensitizer is different from the activator are more efficient and more complicated.

Auzel was apparently the first to discover the sensitization of Er^{3+} and Tm^{3+} by Yb^{3+} (in $Na_{0.5}Yb_{0.5}WO_4$), and he advanced a model for excitation that can best be described as a successive transfer model, which requires three transfers from excited Yb^{3+} ions to a Tm^{3+} ion to raise it to the $^1G_4$ luminescing level.[5] He had previously proposed a two-transfer model for Er^{3+} in the same material.[6] Ovsyankin and Feofilov[7] independently discovered the sensitization of Tm^{3+} by Yb^{3+} (in BaF_2) and advanced the "cooperative sensitization" model, according to which two Yb^{3+} ions in the $^2F_{5/2}$ state simultaneously cross relax with a Tm^{3+} ion in the ground state, raising it to the $^1G_4$ state. Both Auzel[5] and Ovsyankin and Feofilov[7] based their models on data relating the dependence of the luminescence intensity upon the intensity of the flux absorbed by the Yb^{3+} ions, which they claimed was cubic and quadratic, respectively.

Esterowitz *et al.*[8] discovered the sensitization of Ho^{3+} quantum counter action by Yb^{3+} in CaF_2, which they attributed to a single transfer from the Yb^{3+} ion to the Ho^{3+} such that the $^5I_8$-$^5I_6$ transition is bypassed, with further excitation then occurring in the Ho^{3+} ion. They considered a cross relaxation of the Ho^{3+} ion from its $^5S_2$ luminescent level to the $^5I_6$ level with the Yb^{3+}($^2F_{7/2} \rightarrow {}^2F_{5/2}$) transition, but not in the other direction, which would result in a double-transfer process like that found by Auzel for the Yb-Er system.

We present here a series of experiments, made possible by the discovery that the use of the lanthanide trifluoride hosts LaF_3, GdF_3, and LuF_3, and also YF_3 results in greatly increased conversion of near 1 μ radiation to visible luminescence, which indicate that the Auzel,[5] rather than the Ovsyankin and Feofilov[7] or Esterowitz *et al.*[8] mechanisms are operative in the excitation of these (Ho^{3+}, Er^{3+}, or Tm^{3+}) activators. The approach used is to compare the excitation spectra of these materials with their reflectance spectra, and to consider the dependence of the visible luminescence upon (i) the sensitizer concentration for constant excitation conditions, and (ii) on the intensity of the exciting radiation.

THEORETICAL

Since the data presented below will be interpreted on the basis of a successive transfer model rather than one of the other two, analysis of that model is necessary. We will consider first a four-level model requiring three transfers, for the case of Tm^{3+}, operating under steady-state dc excitation, and then will simplify this to obtain a model for only two transfers, which is the case for Ho^{3+} and Er^{3+}. The four-level model is shown in Fig. 1, and only those transitions indicated will be considered. All upward transitions are assumed to be by cross relaxation with the sensitizer ions, and back transfer

[1] N. Bloembergen, Phys. Rev. Letters **2**, 84 (1959).
[2] R. J. Woodward, J. M. Williams, and M. R. Brown, Phys. Letters **22**, 435 (1966).
[3] V. V. Ovsyankin and P. P. Feofilov, Zh. Eksperim. i Teor. Fiz. Pis'ma v Redaktsiyu **3**, 494 (1966) [English transl.: Soviet Phys.—JETP Letters **3**, 322 (1966)].
[4] E. Chicklis and L. Esterowitz, Phys. Rev. Letters **21**, 1149 (1968).
[5] F. Auzel, Compt. Rend. **263B**, 819 (1966).
[6] F. Auzel, Compt. Rend. **262B**, 1016 (1966).
[7] V. V. Ovsyankin and P. P. Feofilov, Zh. Eksperim. i Teor. Fiz. Pis'ma v Redaktsiyu **4**, 471 (1966) [English transl.: Soviet Phys.—JETP Letters **4**, 317 (1966)].
[8] L. Esterowitz, J. Noonan, and J. Bahler, Appl. Phys. Letters **10**, 126 (1967).

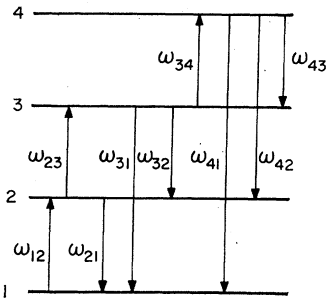

FIG. 1. Four-level system with transitions leading to IRQC action by energy transfer indicated.

will be neglected as the level spacings are at least 1500 cm^{-1} less than the Yb^{3+} ($^2F_{7/2} \rightarrow {}^2F_{5/2}$) separation, which is approximately 10^4 cm^{-1}. Similarly, transfer can only result in excitation from the jth level to the $(j+1)$st. ω_{ij} represents the transition probability per unit time from the ith to the jth levels, and for $i>j$ includes nonradiative processes. N_i is the population of the ith level, and the total number of ions is N. The resulting rate equations are then

$$dN_1/dt = -N_1\omega_{12}+N_2\omega_{21}+N_3\omega_{31}+N_4\omega_{41}, \quad (1)$$

$$dN_2/dt = N_1\omega_{12}-N_2(\omega_{21}+\omega_{23})+N_3\omega_{32}+N_4\omega_{42}, \quad (2)$$

$$dN_3/dt = N_2\omega_{23}-N_3(\omega_{31}+\omega_{32}+\omega_{34})+N_4\omega_{43}, \quad (3)$$

$$dN_4/dt = N_3\omega_{34}-N_4(\omega_{43}+\omega_{42}+\omega_{41}), \quad (4)$$

$$N = N_1+N_2+N_3+N_4. \quad (5)$$

The steady-state solution for the fluorescence intensity from state 4 to state 1 is given by

$$\begin{aligned} I_{41} = N_4\omega_{41} = N\omega_{12}\omega_{23}\omega_{34}\omega_{41}(&\omega_{12}\omega_{34}\omega_{23}+\omega_{12}\omega_{34}\omega_{41} \\ &+\omega_{12}\omega_{32}\omega_{41}+\omega_{12}\omega_{41}\omega_{31}+\omega_{12}\omega_{34}\omega_{42}+\omega_{12}\omega_{32}\omega_{42} \\ &+\omega_{12}\omega_{42}\omega_{31}+\omega_{12}\omega_{43}\omega_{32}+\omega_{12}\omega_{43}\omega_{31}+\omega_{12}\omega_{23}\omega_{41} \\ &+\omega_{12}\omega_{23}\omega_{42}+\omega_{12}\omega_{23}\omega_{43}+\omega_{23}\omega_{31}\omega_{43}+\omega_{23}\omega_{31}\omega_{42} \\ &+\omega_{23}\omega_{31}\omega_{41}+\omega_{34}\omega_{21}\omega_{42}+\omega_{34}\omega_{21}\omega_{41}+\omega_{21}\omega_{42}\omega_{32} \\ &+\omega_{21}\omega_{42}\omega_{31}+\omega_{21}\omega_{41}\omega_{32}+\omega_{21}\omega_{41}\omega_{31}+\omega_{21}\omega_{43}\omega_{32} \\ &+\omega_{21}\omega_{43}\omega_{31})^{-1}. \end{aligned} \quad (6)$$

Now since all ω_{ij} $(i<j)$ are dependent upon the number of excited sensitizer ions, the denominator can be simplified by (i) reducing the sensitizer concentration or (ii), reducing the flux which excites them. In either case all but the last six terms in the denominator can be made arbitrarily small so that Eq. (6) reduces to

$$\begin{aligned} I_{41} = N\omega_{12}\omega_{23}\omega_{34}\omega_{41}(&\omega_{21}\omega_{42}\omega_{32}+\omega_{21}\omega_{42}\omega_{31}+\omega_{21}\omega_{41}\omega_{32} \\ &+\omega_{21}\omega_{41}\omega_{31}+\omega_{21}\omega_{43}\omega_{32}+\omega_{21}\omega_{43}\omega_{31})^{-1}. \end{aligned} \quad (7)$$

If we now set $\omega_{12}=FN_s\alpha_{12}$, etc., where F is the flux absorbable by the sensitizers and N_s is their concentration, and α_{12} represents the cross-relaxation coupling, we see that Eq. (7) varies cubically in both F and N_s.

For arbitrarily high flux intensities, the first term in Eq. (6) will predominate and I_{41} will be independent of F, and at intermediate intensities linear and/or quadratic terms will control, and hence that I_{41} will vary in dependence upon F from cubic to independent. The values of flux actually required will depend on many factors, including oscillator strengths for sensitizer and activator absorption, which are related to α_{ij} in a manner depending upon the mechanism involved in the transfer, i.e., dipole-dipole, dipole-quadrupole, or exchange; and the nonradiative relaxation rates from any of the excited states, both multiphonon and activator-activator cross relaxation, which will increase ω_{ij} $(i>j)$ beyond the value due to radiative decay. α_{ij} and the radiative and nonradiative decay rates are all affected by the crystal structure.

Equations (1)–(5) can be solved for fluorescence from one of the intermediate states, say from state 3 to state 1 to obtain

$$\begin{aligned} I_{31} = N_3\omega_{31} = N\omega_{12}\omega_{23}\omega_{31}\{&\omega_{21}(\omega_{31}+\omega_{32})+\omega_{12}\omega_{32}+\omega_{12}\omega_{31} \\ &+\omega_{23}\omega_{31}+\omega_{21}\omega_{24}-[\omega_{43}\omega_{34}(\omega_{21}+\omega_{12})]/ \\ &(\omega_{41}+\omega_{42}+\omega_{43})+\omega_{12}(\omega_{23}+\omega_{34})\}^{-1}. \end{aligned} \quad (8)$$

For low-flux or sensitizer concentrations this reduces to

$$I_{31} = NF^2N_s^2\alpha_{12}\alpha_{23}\omega_{31}\omega_{21}(\omega_{31}+\omega_{32})^{-1}, \quad (9)$$

so that I_{31} should be proportional to the square of N_s and F. For high excitation intensity, the term $\omega_{12}\omega_{23}$ will control in the denominator in Eq. (8) (the term $\omega_{12}\omega_{34}$ is canceled by part of the preceding term) and I_{31} will be independent of F. The result I_{31}' for a three-level system can be obtained from Eq. (8) by letting all terms in ω_{i4} or ω_{4j} go to zero in the same manner,

$$\begin{aligned} I_{31}' = N\omega_{12}\omega_{23}\omega_{31}[&\omega_{21}(\omega_{31}+\omega_{32}) \\ &+\omega_{12}(\omega_{32}+\omega_{23}+\omega_{31})+\omega_{23}\omega_{31}]^{-1}. \end{aligned} \quad (10)$$

For a three-level system in which absorptions are made in the activator as well as the sensitizer we replace ω_{12} and ω_{23} by $\omega_{12}+\omega_{12}'$, $\omega_{23}+\omega_{23}'$, respectively, where ω_{12}' and ω_{23}' represent nontransfer excitations. Equation (10) then becomes

$$I_{31}' = \frac{N(\omega_{12}+\omega_{12}')(\omega_{23}+\omega_{23}')\omega_{31}}{[\omega_{21}(\omega_{31}+\omega_{32})+\omega_{12}(\omega_{32}+\omega_{23}+\omega_{31})+\omega_{23}\omega_{31}]} \quad (11)$$

and, for low sensitizer concentrations (for low excitation intensities ω_{12}, ω_{23} will still predominate over ω_{12}', ω_{23}' since the sensitizer has greater oscillator strength than the activator), this reduces to

$$I_{31}' = \frac{N'\omega_{31}(\omega_{12}'\omega_{23}'+\omega_{12}'\omega_{23}+\omega_{12}\omega_{23}')}{[\omega_{21}(\omega_{31}+\omega_{32})]} \quad (12)$$

so that at low sensitizer concentrations I_{31}' will be independent of N_s and at somewhat greater concentrations will be linear in N_s.

EXPERIMENTAL

A. Materials Preparation

The most comprehensive and reliable data concerning the crystal-chemical relationships of the trivalent rare-earth fluorides were published by Thoma and Brunton[9] and is best summarized by referring to Fig. 2 which has been reproduced from their paper. The fluorides from Sm to Lu (also Y) undergo a rapid, reversible orthorhombic $\rightleftarrows$ hexagonal (O $\rightleftarrows$ H) phase transformation at elevated temperatures. No such dimorphism was detected from La to Nd. The high-temperature hexagonal structures from Sm to Ho are isotopic with LaF_3, whereas the hexagonal modifications between Er and Lu are isotopic with the high-temperature hexagonal modification of YF_3 (0 $\rightleftarrows$ H at 1052°C, mp at 1144°C).

In the present investigation polycrystalline-powder samples of the fluorides of La, Y, Gd, and Lu activated with Yb^{3+} and Er^{3+}, Ho^{3+}, or Tm^{3+} were synthesized by coprecipitating the oxalates from nitric acid solutions of the oxides, followed by decomposition of the oxalates to the oxides at 750°C in air, and finally by reaction of the oxides with anhydrous HF at temperatures of 900–1100°C. The reactions were carried out in a platinum container in a platinum tube furnace. This procedure was necessary to ensure the complete absence of oxide or oxyfluoride phases in the powders, since these were found to be orders of magnitude inferior in IRQC action when compared with the fluorides. This procedure led to well-crystallized single-phase powders as determined by standard powder x-ray diffraction techniques. Because of the similarity in crystal chemistry among the fluorides of Y, Gd, Lu, Yb, Er, and Tm, complete crystalline solubility is expected between the orthorhombic modifications of the fluorides of these elements. The Goldschmidt ionic radii of triply positive rare earths for these elements range from 1.11 Å for Gd^{3+} to 0.99 Å for Lu^{3+}. La^{3+} ($r=1.22$ Å) is considerably larger and it was found that the crystalline solubility of YbF_3 in LaF_3 was limited to about 18–20 mole % at 1000°C. LaF_3:Er composition containing more than this amount of YbF_3 were found to contain two phases from a determination of the lattice parameters of LaF_3: Yb, Er solid solutions.

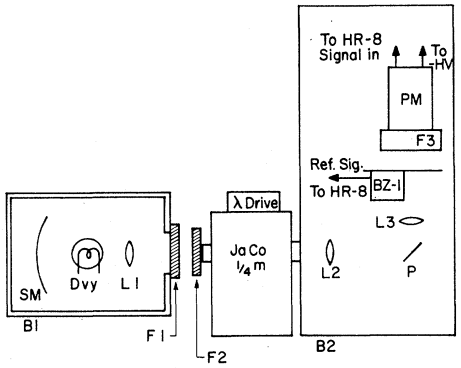

FIG. 3. Schematic of excitation apparatus. B1, B2, light-tight boxes. F1, F2, infrared passing filters; F3, luminescence-isolating filter. L1, L2, collecting and focusing lenses for exciting radiation; L3,-luminescence-collecting lens. SM, spherical mirror; DVY, 650 W G.E. quartz-iodine-tungsten lamp. JaCo, Jarrell-Ash ¼ m monochrometer; BZ-1, PAR 400 Hz chopper. PM, EMI 9558 QB photomultiplier.

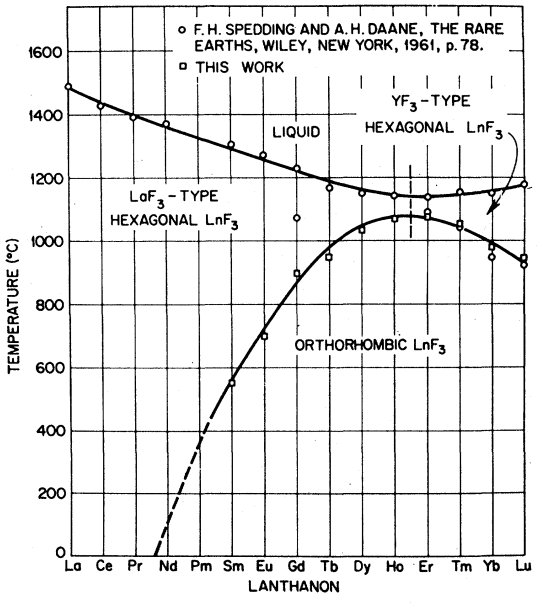

FIG. 2. Dimorphism among the rare-earth trifluorides (see Ref. 9).

[9] R. E. Thoma and G. D. Brunton, Inorg. Chem. **5**, 1937 (1966).

B. Apparatus and Procedure

The excitation spectra were taken on the apparatus shown schematically in Fig. 3. The DVY 650 W quartz-iodine-tungsten lamp was operated dc to avoid any lifetime effects and was powered by a Sorenson DCR 150–10 A supply. A spherical mirror behind the lamp refocused the light back on the lamp and a lens then focused the light on the entrance slit of a Jarrell-Ash ¼-m monochromator, which was covered by a red-pass filter (Corning 2-58) which eliminated second-order visible light from the 590-l/mm grating. The lamp, mirror, and lens were all enclosed in a light tight box sealed by Optics Technology 650-nm-long wavelength pass (650LP) and 550 short pass (550SP) filters. The SP filter transmits from 350 to 580 nm and again from 800 nm to the glass cutoff. The combination had an optical density of 2 or more for wavelengths below 780 nm. A second lens focused the exciting radiation on the phosphor powder which was pressed into a plaque, and the luminescence was focused by another lens through a PAR BZ-1 chopper on the photocathode of an EMI 9558QB photomultiplier, which was optically sealed to Corning 4–97 and Optics Technology 550 SP filters so that only blue and green light could reach the cathode.

The entire detection system and sample were placed in a light-tight box to which the exit slit of the excitation monochromator was sealed, so that no stray light from the source could reach the detector. The photomultiplier signal was then synchronously amplified with a reference signal from the chopper in a PAR HR-8 lock-in amplifier and the output recorded against wavelength. To normalize the excitation curves a Reeder thermocouple was placed with its junction in the phosphor position and the signal, proportional to incident energy, was recorded against wavelength. Then using the intensity dependence, which was obtained in a manner described below, the excitation curves were divided by the appropriate power of the ratio of actual excitation energy per unit wavelength interval to normalize to constant energy input.

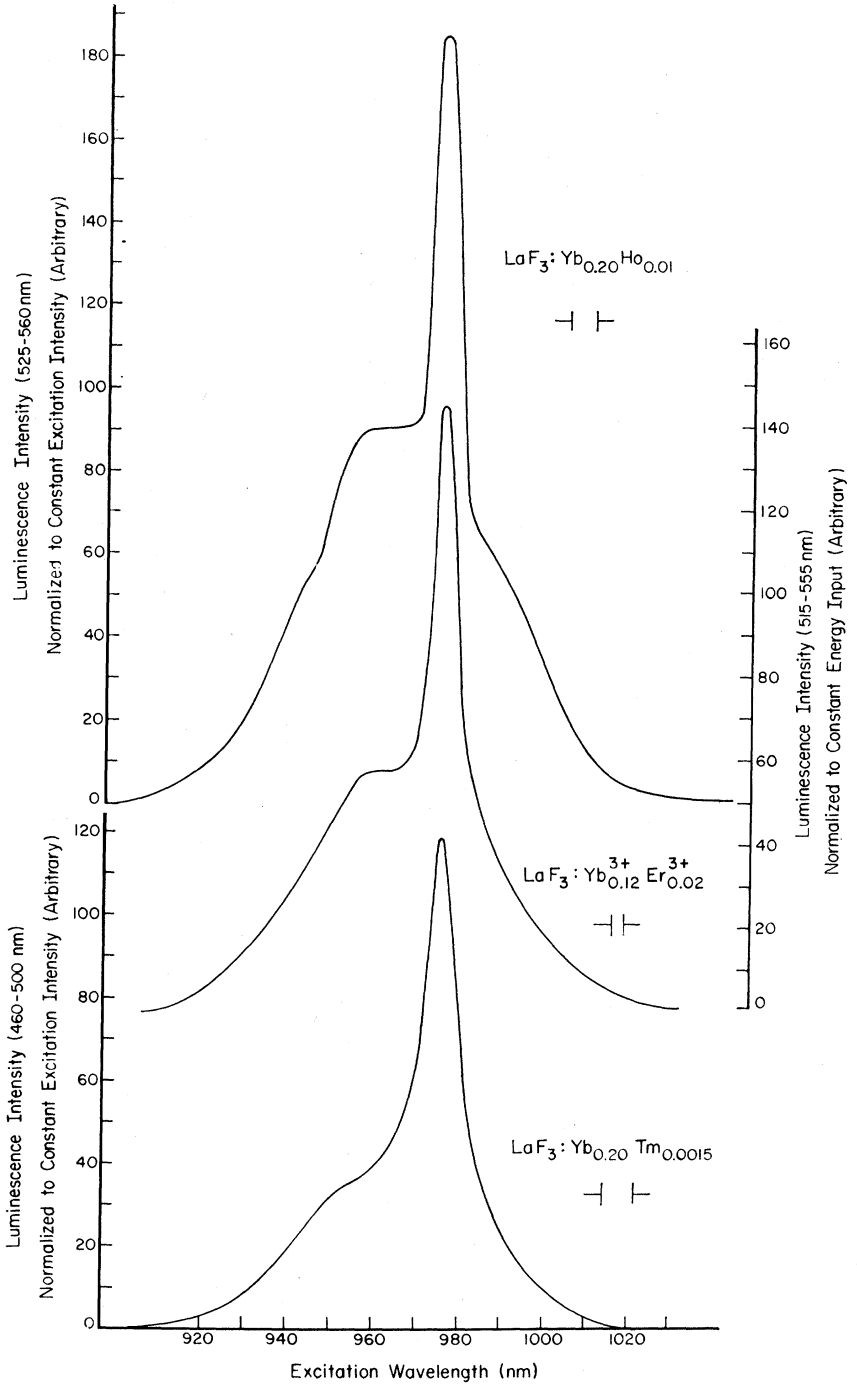

FIG. 4. Infrared excitation spectrum for $(^2H_{11/2}$ and $^4S_{3/2} \rightarrow {}^4I_{15/2})Er^{3+}$ luminescence in LaF_3:Yb, Er, for the $(^1G_4 \rightarrow {}^3H_6)Tm^{3+}$ luminescence in LaF_3:Yb, Tm and for the $(^5F_4$ and $^5S_2 \rightarrow {}^5I_8)Ho^{3+}$ luminescence in LaF_3:Yb, Ho. The excitation spectral band widths are indicated. Sample temperature was nominally 300°K.

The intensity-dependence data were obtained in a similar setup, but with certain additions: A Wratten 87B filter was placed at the excitation monochromator exit slit (which was now 10 mm, as compared to the $\frac{1}{2}$- or 1-mm slits used for obtaining the excitation spectra), and a Bausch and Lomb (BL) 33-86-02 monochromator was now between the phosphors and the photomultiplier. An Optics Technology 500 SP filter was placed between the BL and the photomultiplier for measurements on Tm^{3+}-activated materials, and a Corning 4–96 filter for the Er^{3+} materials. BL neutral density filters, whose optical density in the infrared was measured on a Cary 14 spectrometer, were placed in the exciting beam on either or both sides of

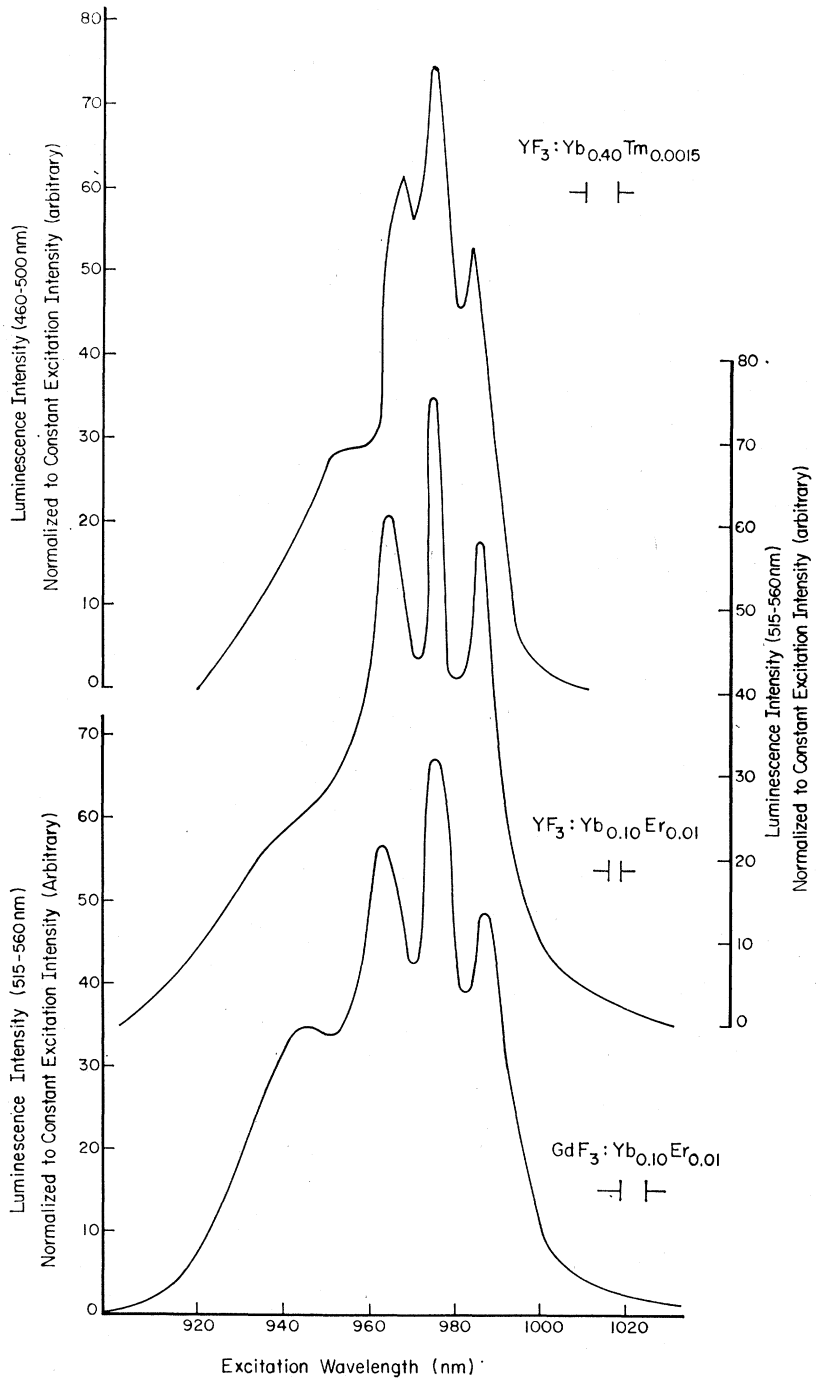

FIG. 5. Infrared excitation spectrum for Er^{3+} luminescence in YF_3:Yb, Er, and GdF_3:Yb, Er, and for Tm^{3+} luminescence in YF_3:Yb, Tm.

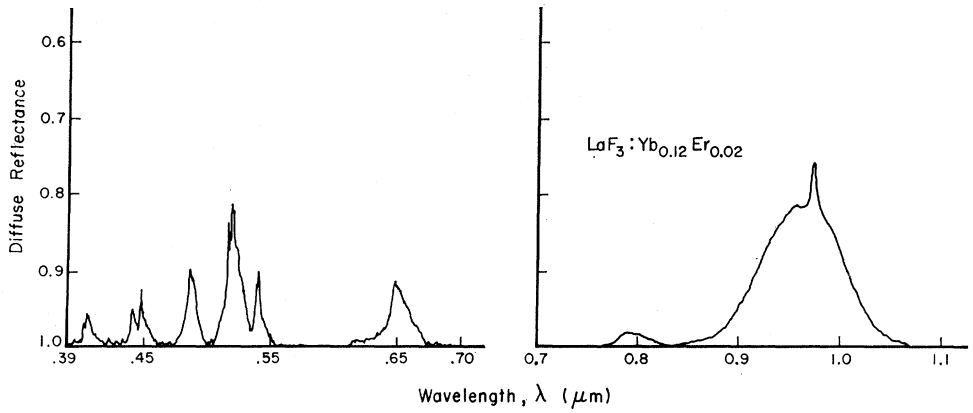

FIG. 6. Diffuse reflectance of LaF_3:Yb, Er compared to LaF_3. The spectral-slit width was 12 Å or better.

the excitation monochrometer. The signal at the luminescence wavelength was then noted for each combination of o.d. filters.

The temperature-dependence data were obtained by mounting the samples in a 1/32-in.-deep plaque on the end of a cold finger in a Sulfrian cryostat. The cold finger was thermally isolated from the cold reservoir but connected by a thermal switch consisting of copper coils through which coolant from the reservoir could be pumped to achieve any desired temperature below room temperature. An electrical heater in the cold finger permitted measurements up to 50°C. For measurements at temperatures above this the samples were mounted in a hot cell described by Davis and Datta.[10] In these measurements excitation was by the DVY source through an Optics Technology 650 LP and 550 SP filters and a Corning 2-58 filter. The emission was recorded against wavelength on a spectroradiometer similar to that described by Brown[11] which records energy nm^{-1} cm^{-2} against wavelength, using a spectral bandwidth of 1 nm. The total light output at a given temperature was then obtained by mechanical integration of the curves. Temperatures were measured using a potentiometer, and an iron constant thermocouple which was in good contact with the sample block. Data were taken both from high-to-low and low-to-high temperatures and then averaged.

Relative efficiency measurements on various phosphors were made using the spectroradiometer for detection and using the DVY source and either a Jarrell-Ash monochrometer or an Optics Technology 1-μm interference filter set at the proper angle to achieve a narrow band of radiation near 0.97 μm. The samples were mounted in identical plaques in a wheel to achieve identical measuring conditions.

The diffuse reflectances of these materials were obtained on Cary 14's equipped with diffuse-reflectance (ring-collector) accessories. For measurements in the infrared, one of the machines was modified so that the PbS cell was mounted over the photomultiplier, and thus, only monochromatic light reached the samples.

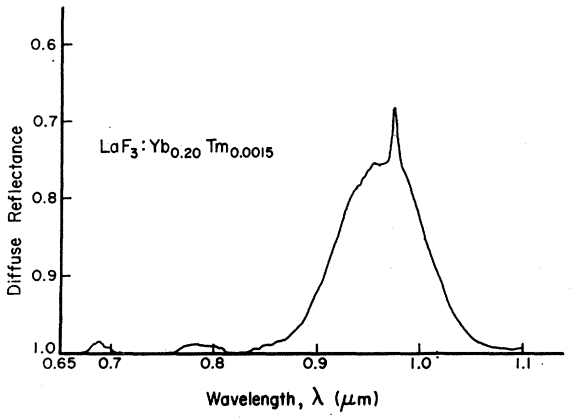

FIG. 7. Diffuse reflectance of LaF_3:Yb, Tm compared to LaF_3.

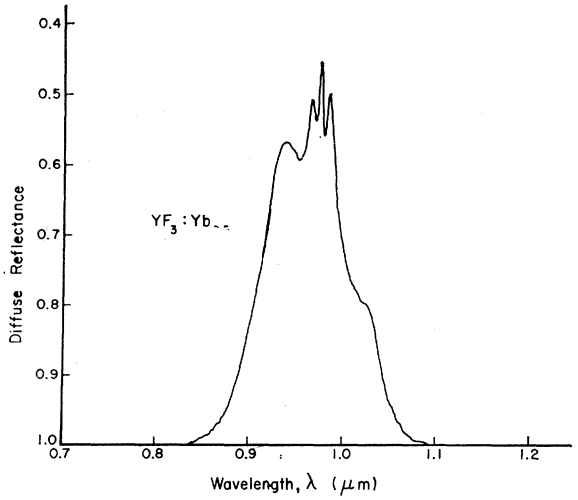

FIG. 8. Diffuse reflectance of YF_3:Yb compared to YF_3.

[10] T. S. Davis and R. K. Datta, Trans. AIME **242**, 714 (1968).
[11] R. L. Brown, Illum. Engr. **61**, 230 (1966).

RESULTS AND DISCUSSION

The excitation spectra for LaF_3:Yb^{3+}, RE^{3+} where RE^{3+} is Er^{3+}, Ho^{3+}, and Tm^{3+} are shown in Fig. 4. Note the similarity of the spectra, especially for Ho^{3+} and Er^{3+}. The Er^{3+} material was 18 times as efficient as the Ho^{3+} material, so that narrower slits could be used for the Er^{3+} sample and still have a better signal to noise ratio. Hence, the Er^{3+} data are felt to be more correct. The much lower efficiency of the Tm^{3+} material required the use of still wider slits, which enhances the broad band at the expense of the narrow band centered near 975 nm. Hence, had it been possible to use as narrow slits for these as for other materials, the wide band would be reduced compared to the narrow band. The excitation spectra of YF_3:Yb, Er and YF_3:Yb, Tm are shown in Fig. 5. Again the difference is felt to be due to increased spectral-band width and decreased signal to noise for the Tm^{3+} sample compared to the Er^{3+} sample. The YF_3 materials are somewhat less efficient than LaF_3 materials. Figure 5 also shows the excitation spectrum for GdF_3:Yb, Er which is seen to be similar to the YF_3 spectra. The excitation spectra for Lu and YbF_3 were not taken, but are expected to be similar to the YF_3 data, since GdF_3, YbF_3, and LuF_3 all have the YF_3 structure, the only difference being lattice-parameter variations.

The reflectance spectra for some of these materials are shown in Figs. 6–8, and 10. The resemblance between the excitation spectra for the YF_3 and GdF_3 materials and the YF_3:Yb^{3+} reflectance is apparent, and by comparing the reflectance in the 900–1050 nm region for the LaF_3 materials it is at once obvious that in both cases the broad band plus peak(s) are due to Yb^{3+}.

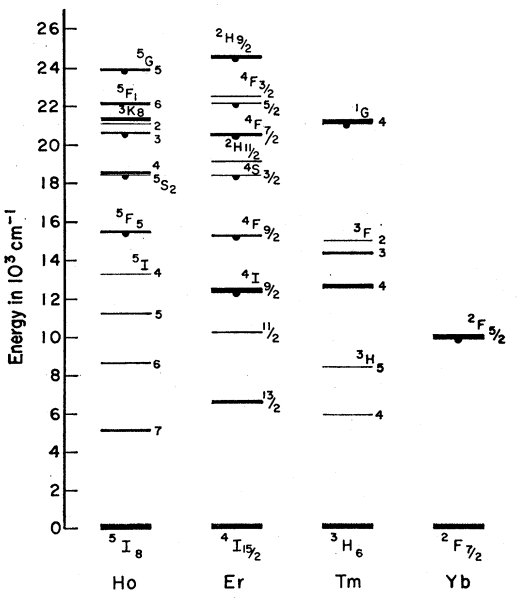

FIG. 9. Energy levels of Ho^{3+}, Er^{3+}, Tm^{3+}, and Yb^{3+} (after Diecke and Crosswhite, Ref. 12).

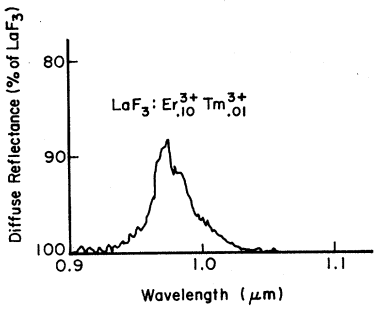

FIG. 10. Diffuse reflectance of LaF_3:Er, Tm compared with LaF_3.

Since, as Fig. 9 shows,[12] Tm^{3+} has no energy levels near 10^4 cm^{-1}, and also no spacings of this magnitude, it is obvious that excitation of Tm^{3+} ions are accomplished by energy transfer from Yb^{3+}. However, both Er^{3+} and Ho^{3+} have spacings of this magnitude [($^4I_{15/2}$ to $^4I_{11/2}$) and ($^4I_{11/2}$ to $^4F_{7/2}$) for Er^{3+} and ($^5I_6$ to $^5S_2$ and $^5F_4$) for Ho^{3+})] and it is possible for these ions to be excited to the luminescent state by only one transfer with the other excitation occurring in the activator ion. One method of deciding which process is predominant in the lanthanide fluorides is to compare the products of the reflectance spectra to the excitation spectra. For diffuse-reflectance measurements, $1-R_j=A_j$, where R_j is the diffuse reflectance for the jth transition, and A_j the absorptance, when the powder layer is "infinitely thick." The plaques used were $\frac{1}{16}$ in. deep and the average particle size was approximately 10 μ, so that the assumption is reasonable. If we then assume that the transitions involved are denoted by m and n, the excitation spectrum should strongly resemble A_mA_n. It was possible to measure the reflectance spectrum of the ($^4I_{15/2}$ to$^4I_{11/2}$)Er^{3+} transition, shown in Fig. 10, but not the other Er^{3+} or the Ho^{3+} transition, as they are from excited states. It was necessary to use a sample doped to 10% Er^{3+} in order to have sufficient absorptance that meaningful data could be taken, and the reflectance of this material in the visible was compared to the 2% Er^{3+} material to see if the band was broadened by ion-ion interactions at this higher-doping level. Such broadening was found to be negligible. The width of the Er^{3+}($^4I_{11/2}$–$^4F_{7/2}$) transition was expected to be no greater than the ($^4I_{15/2}$–$^4I_{11/2}$) transition. Figure 11 shows the correspondence between various powers of the Yb^{3+} absorptance, the product of the Yb^{3+} absorptance and the Er^{3+} ($^4I_{15/2}$ to $^4I_{11/2}$) absorptance, and the excitation spectrum for LaF_3:Yb, Er^{3+}. The lack of similarity of band shape for the product curve and the strong similarity between the cube of the Yb^{3+} absorptance indicates that the ($^4I_{15/2}$–$^4I_{11/2}$) transition is not significantly involved, and that in both Er^{3+} and Ho^{3+} (from the similarity of the excitation spectra, Fig. 4) both transitions are

[12] After G. H. Dieke and H. M. Crosswhite, Appl. Optics 2, 675 (1963).

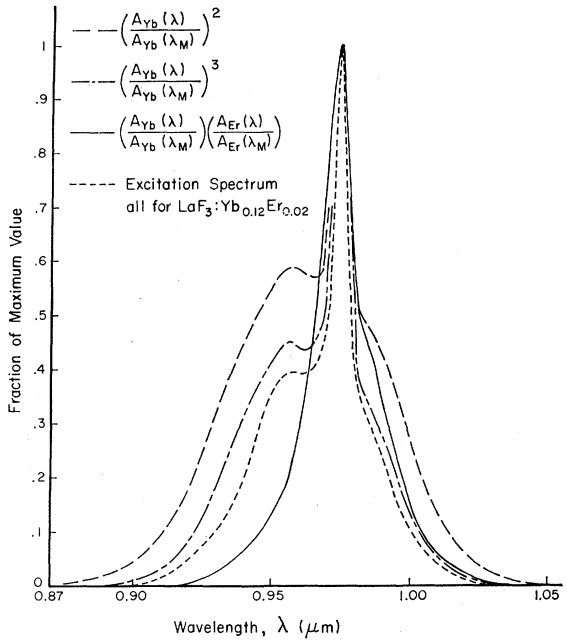

FIG. 11. Comparison of the excitation spectrum of LaF_3:Yb, Er with powers of the Yb^{3+} absorptance and the Yb^{3+}—Er^{3+} product. $A_{Yb}(\lambda)/A_{Yb}(\lambda_M)$ is the normalized $Yb^{3+}(^2F_{7/2} \rightarrow {}^2F_{5/2})$ absorptance, and $A_{Er}(\lambda)/A_{Er}(\lambda_M)$ is the normalized Er^{3+} ($^4I_{15/2} \rightarrow {}^4I_{11/2}$) absorptance.

accomplished by transferred energy. The fact that the cube rather than the square of the Yb^{3+} absorptance resembles the excitation spectrum most can be explained by invoking the intensity dependence of the efficiency of the material: Since, as will be shown later, the luminescence dependence is quadratic upon the excitation intensity, that light absorbed by the Yb^{3+} ions in regions of low excitation intensity will not result in luminescence from the visible emitting states, but from the $^4I_{11/2}$ state as the interval between transfers will exceed the lifetime of that state.

A second method of ascertaining whether the energy is absorbed only in the Yb^{3+} ions or also in the activator ions is to examine the efficiency versus sensitizer concentration for the low sensitizer-concentration range. Equation (11) predicts: (i) If no transfers are effected, the efficiencies will be independent of the sensitizer concentrations; (ii) if the process of one

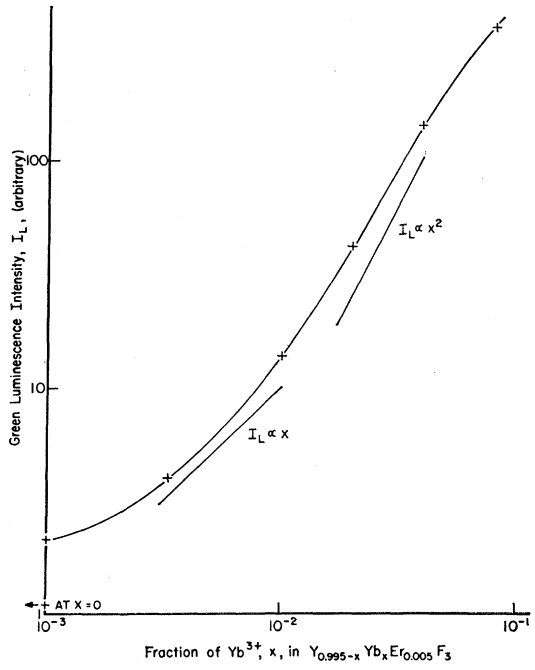

FIG. 12. Variation of Er^{3+} ($^2H_{11/2}$ and $^4S_{3/2} \rightarrow {}^4I_{15/2}$) luminescence intensity with sensitizer concentration for infrared (≈ 1 μ) excitation.

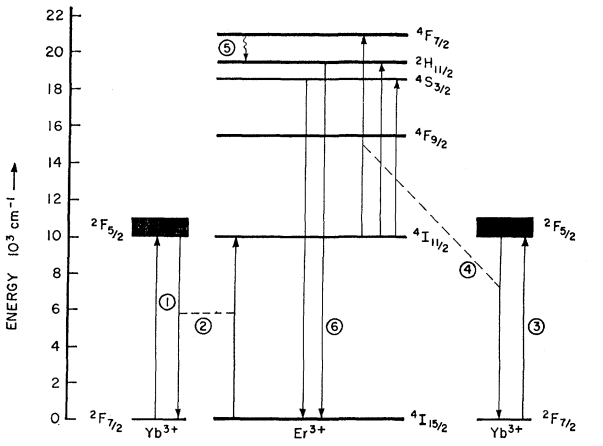

FIG. 13. Mechanism of excitation of the green luminescence in Er^{3+}: (1) Absorption of an IR photon by a Yb^{3+} ion; (2) transfer of this energy from the Yb^{3+} ion to the Er^{3+} ion, where it is stored while another IR photon is absorbed; (3) and transferred (4) to the Er^{3+} ion which then relaxes (5) to the luminescent state prior to the emission of luminescence (6). Back transfer from Er^{3+} to Yb^{3+} and nonradiative relaxation in the Er^{3+} ion from the $^4I_{11/2}$ level to lower levels (not shown), or from luminescent level to lower levels, is not indicated. Step (4) may be directly to one of the luminescent levels, so that step (5) may not be required.

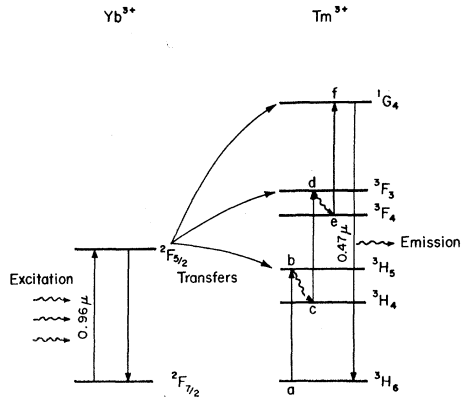

FIG. 14. Auzel's successive-transfer model for the sensitized excitation of Tm^{3+} ions by near 1-μm radiation (after Auzel).

transfer and one internal excitation is dominant, it will be linear; and (iii) if two transfers are required it will be quadratic in the sensitizer concentration. Figure 12 shows the variation of efficiency with Yb^{3+} concentration in $YF_3:Yb^{3+}$, $Er_{0.005}{}^{3+}$, and it is seen that for concentrations near 0.6% it is linear, and for concentrations between 2 and 5% it is quadratic. At low concentrations it becomes independent of Yb^{3+} concentration, as both transitions occur in the Er^{3+} ion.

Hence, it appears on the basis of the reflectance, excitation, and concentration-dependence spectra, that the mechanism shown in Figure 13, which requires two transfers, rather than that of Esterowitz *et al.*,[8] best explains the excitation processes in Ho^{3+} and Er^{3+}.

At this point the possibility remains that the excitation of Ho^{3+} and Er^{3+} is achieved by the simultaneous "cooperative sensitization" process of Ovsyankin and Feofilov[7] rather than the successive-transfer model indicated above. To decide this point the excitation processes of Tm^{3+} were investigated, as this case is much more definitive, since the successive-transfer model of Auzel[5] shown in Fig. 14 requires three transfers, while the model of Ovsyankin and Feofilov[7] only

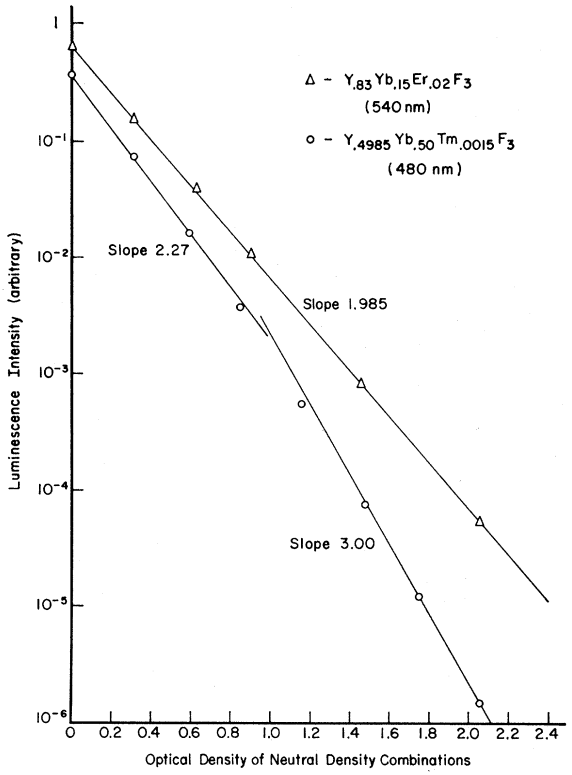

FIG. 15. Intensity dependence of visible luminescence I_L upon intensity of infrared (≈ 1 μm) excitation I_E. The intensity of the IR beam was attenuated by neutral-density filter combinations whose values are shown as the abscissa. Thus, for an o.d. of the 1 the excitation intensity was 10% of that for o.d. = 0. No absolute measurements of the IR intensity was made. The slope indicates n in $I_L \propto I_E{}^n$.

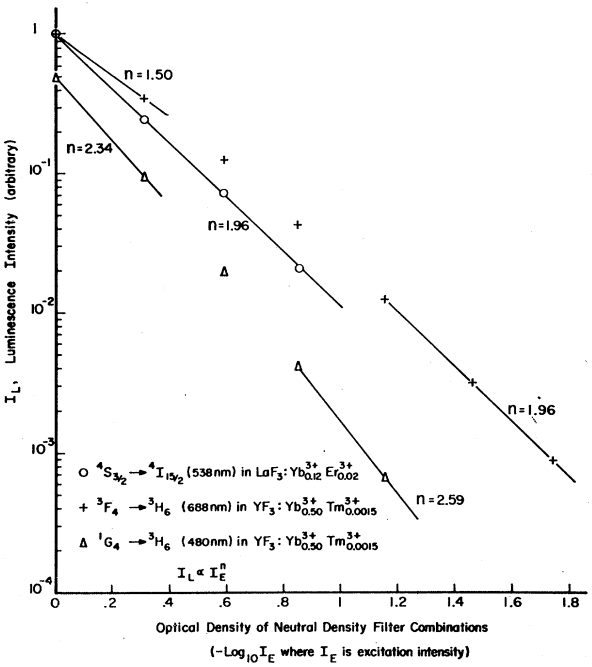

FIG. 16. Intensity dependence of visible (538 nm in Er^{3+} and 480 nm in Tm^{3+}) and intermediate state (688 nm in Tm^{3+}) luminescence upon excitation intensity. The optical density of the neutral density filter combinations used to attenuate the IR beam is the abscissa.

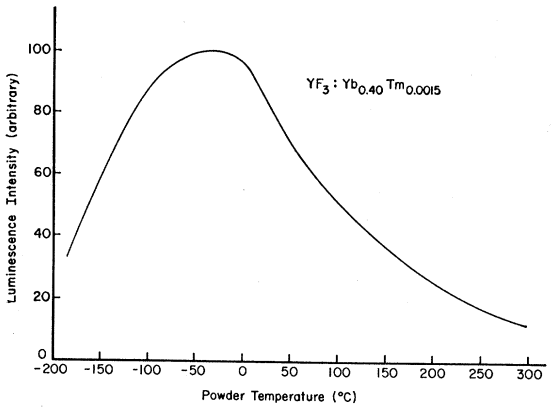

FIG. 17. Dependence of total ($^1G_4 \rightarrow {}^3H_6$)$Tm^{3+}$ luminescence with temperature.

requires two. Hence, it should be possible to resolve the question by examining the intensity-dependence data. Figures 15 and 16 show the intensity dependence of both Er^{3+} and Tm^{3+} materials, and indicate the relationship of the luminescence intensity I_L to excitation intensity I_E through the formula $I_L \propto I_E{}^n$. The Er^{3+} materials were excited under the same conditions as the Tm^{3+} materials shown in the same figures, to determine if the decrease in slope at high excitation intensity was due to saturation of the intermediate levels according to Eq. (6) or due to heating effects from the exciting beam. It is evident that the Er^{3+} $^4I_{11/2}$

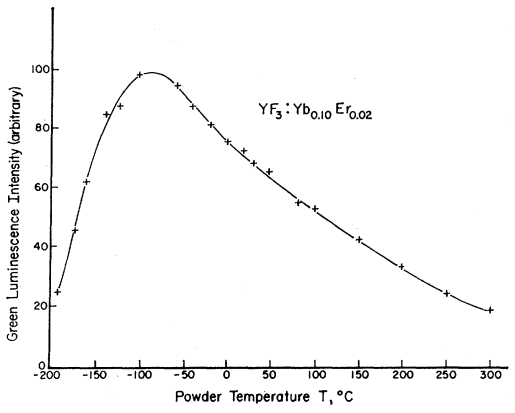

FIG. 18. Dependence of total green Er^{3+} luminescence with temperature.

level is not saturating, nor is the phosphor heating appreciably. By recording the Tm^{3+} luminescence intensity as the o.d. of the filters was sharply decreased to 0 or 0.3 at most, it was obvious that the Tm^{3+}-activated materials were heating, in accordance with the temperature dependence shown in Fig. 17 as the signal decreases from its initial value to about 90 to 95% of that value over a several second period. The temperature dependences of Ho^{3+} and Er^{3+} materials are shown in Figs. 18 and 19 to show they behave similarly. In the case of Fig. 16, where the intensity dependence of the luminescence from the second-storage level is shown, saturation is also evident. Indeed, were the simultaneous-transfer model the correct one, the intensity dependence of this level should be the same as that for the 480-nm luminescence, as all the intermediate levels are bypassed and could only be populated from the $^1G_4$ level.

The concentration dependence of $GdF_3:Yb^{3+}$, Tm^{3+}- is shown in Fig. 20 and in the low-concentration range the dependence of phosphor efficiency on Yb^{3+} concentration is in definite agreement with Eq. (7). Thus, it appears that the excitation process of Auzel,[5] requiring three transfers, is indeed the dominant process in

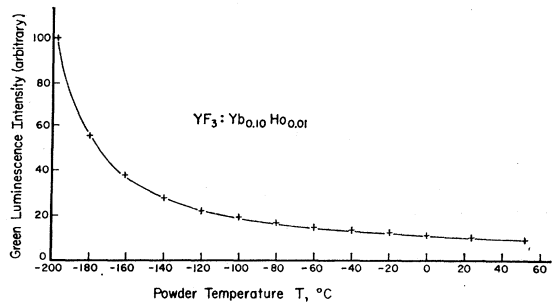

FIG. 19. Dependence of total green Ho^{3+} luminescence with temperature.

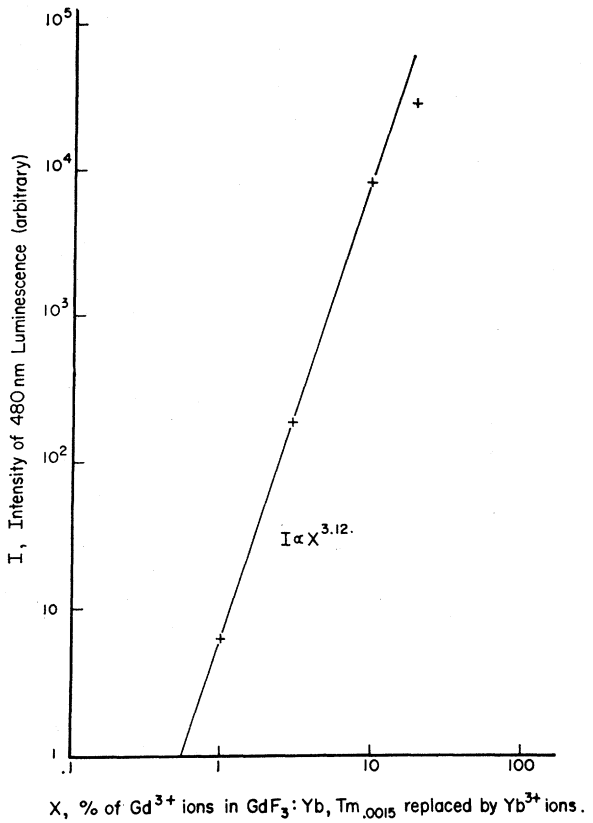

FIG. 20. Dependence of $Tm^{3+}(^1G_4 \rightarrow {}^3H_6)$ luminescence in GdF_3:Yb, Tm with Yb^{3+} concentration.

Tm^{3+} materials, and by extension and also by comparison of the spike to broad-band contributions to the excitation spectra of LaF_3:Yb, Er; LaF_3:Yb, Tm; and LaF_3:Yb, Ho that in the lanthanide fluorides the successive-transfer model accounts for the experimental observations. The intensity dependence seen by Ovsyankin and Feofilov[7] can be attributed to the greatly inferior efficiency of the BaF_2:Yb, Tm material they used, which would require such high excitation intensities to observe the phenomenon that both heating effects and population saturation would lead to an intensity dependence which could be regarded as quadratic. Studies made on BaF_2:Yb, Tm powders by the present authors revealed results consistent with those found for the landanide trifluoride materials.

ACKNOWLEDGMENTS

The authors are greatly indebted to Dr. R. M. Potter, Dr. T. S. Davis, and Dr. E. F. Apple for valuable discussion; and to Dr. Davis and Dr. J. Marquisee, L. V. Triozzi, Miss E. J. Wilson, and Mrs. B. Burts for assistance in the measurements and preparation of materials.